Advances in Computational Design, *Vol. 8, No. 4 (2023) 327-351*
https://doi.org/10.12989/acd.2023.8.4.327

Multi-objective structural optimization of spatial steel frames with column orientation and bracing system as design variables

Cláudio H. B. de Resende*[1], Luiz F. Martha[2], Afonso C. C. Lemonge[3], Patricia H. Hallak[3], José P. G. Carvalho[4] and Júlia C. Motta[5]

[1]Postgraduate Program of Civil and Environmental Engineering, Pontifical Catholic University of Rio de Janeiro
[2]Department of Civil and Environmental Engineering, Pontifical Catholic University of Rio de Janeiro
[3]Department of Applied and Computational Mechanics - Federal University of Juiz de Fora
[4]Postgraduate Program of Civil Engineering - Federal University of Rio de Janeiro
[5]Postgraduate Program of Civil Engineering - Federal University of Juiz de Fora

(Received August 16, 2023, Revised November 8, 2023, Accepted November 23, 2023)

Abstract. This article explores how multi-objective optimization techniques can be used to design cost-effective and structurally optimal spatial steel structures, highlighting that optimizing performance can be as important as minimizing costs in real-world engineering problems. The study includes the minimization of maximum horizontal displacement, the maximization of the first natural frequency of vibration, the maximization of the critical load factor concerning the first global buckling mode of the structure, and weight minimization as the objectives. Additionally, it outlines a systematic approach to selecting the best design by employing four different evolutionary algorithms based on differential evolution and a multi-criteria decision-making methodology. The paper's contribution lies in its comprehensive consideration of multiple conflicting objectives and its novel approach to simultaneous consideration of bracing system, column orientation, and commercial profiles as design variables.

Keywords: conceptual and feature based design; design optimization; simulation based design; steel structure; structural optimization

1. Introduction

Space steel frames are widely used in various civil engineering applications around the world, and with technological advancements, there is a growing need for more efficient structures that can be designed at a lower cost while also being able to support increasingly taller buildings. However, optimizing such complex designs with only one objective may not be sufficient, and there is a need to consider multiple conflicting objectives. Multi-objective optimization techniques are required to solve these problems and obtain Pareto fronts (PFs) that can provide a set of optimal solutions. From these solutions, the decision-maker (DM) can choose the one that best suits their preferences.

In multi-objective optimization, the goal is to optimize multiple objectives simultaneously while taking into account the trade-offs between them. This involves finding a set of solutions that

*Corresponding author, M.Sc., E-mail: claudiohorta@tecgraf.puc-rio.br

http://www.techno-press.org/?journal=acd&subpage=7 ISSN: 2383-8477 (Print), 2466-0523 (Online)

are not dominated by any other solution, following the dominance concepts described by Deb (2001), known as Pareto optimal solutions. The set of Pareto optimal solutions forms the PF, which provides a range of optimal solutions for the DM to choose from according to his preferences.

Using multi-objective optimization techniques to design space steel frames can lead to more cost-efficient and structurally optimum designs. The PF provides a set of optimal solutions from which the DM can choose, considering their preferences and trade-offs between different objectives, such as cost, weight, and global stability.

The challenge for the DM is to select the solution that best aligns with their preferences, which can be subjective and may vary depending on the context and problem at hand. In the solution extraction process, the DM can manually choose a solution based on their knowledge and experience, or they can use a systematic method such as multi-criteria decision-making (MCDM). MCDM methods allow the designer to incorporate their preferences into the decision-making process by assigning weights to each objective based on their relative importance. The method introduced by Parreiras and Vasconcelos (2005), adopted here, is one such approach, where the designer defines weights for each objective based on their preferences, and a weighted sum approach is used to rank the solutions.

As buildings become taller, the impact of wind on horizontal displacements, the global stability, and the dynamic behavior become significant challenges in structural design. Bracing systems can be used to address these issues. However, selecting the most effective geometric configuration is not a simple task, as there are numerous options commonly adopted in the design of steel frames. In addition, the orientation of the principal axes of inertia of the columns can also impact the global structure behavior, making it difficult to determine the optimal set of orientations for structures of general geometry.

Therefore, finding the best configuration according to the designer's expertise requires careful consideration of multiple variables, including the choice of bracing system and orientation of the columns, among others. This process may not be intuitive and requires the use of advanced optimization techniques to evaluate a large number of design options and select the most effective solution based on multiple conflicting objectives.

In this sense, multi-objective optimization techniques can help designers to consider all relevant variables, such as the weight, cost, stability, and stiffness of the structure, and select the most suitable bracing configuration and column orientation. By using these techniques, designers can obtain a set of Pareto optimal solutions, enabling them to choose the desirable design according to their preferences and objectives. This approach can lead to more cost-efficient and structurally optimum designs while considering all relevant variables.

Structural optimization problems typically focus on minimizing the cost or amount of material used as the single objective. However, in real-world engineering problems, optimizing performance may be just as crucial as minimizing cost. Therefore, it is essential to include multiple objectives in the optimization problem formulations to improve structural performance. In this sense, this paper considers the minimization of maximum horizontal displacement, the maximization of the first natural frequency of vibration, and the maximization of the critical load factor concerning the first global buckling mode of the structure. Considering these objectives in addition to weight minimization, a more comprehensive understanding of the structural system's performance can be achieved, leading to a more efficient and effective design.

Four multi-objective evolutionary algorithms based on differential evolution (DE) introduced by Storn and Price (1995) were adopted to solve the the optimization problems analyzed in this paper: the third evolution step of generalized differential evolution (GDE-3), developed by

Kukkonen and Lampinen (2005); success-history–based adaptive multi-objective differential evolution (SHAMODE); SHAMODE with whale optimization (SHAMODE-WO) presented by Panagant *et al*. (2019); and a multi-objective meta-heuristic with iterative parameter distribution estimation (MM-IPDE), elaborated by Wansasueb *et al*. (2022). Recently, the performance of these algorithms was evaluated by Carvalho *et al*. (2021) in solving multi-objective structural optimization problems concerning two, three, and four conflicting objective functions.

The remainder of this paper is organized as follows. Section 2 shows and lists the related works and the distinct characteristics of the present paper. Section 3 describes the formulation of the multi-objective optimization problems treated in this work. Section 4 explains how the solutions are ranked and extracted from the PF. Section 5 presents the numerical experiments and its results analysis, and finally, the paper ends with concluding remarks and future works in Section 6.

2. Related work

In recent years, the field of structural optimization for steel frames has seen a growing interest in studying bracing systems and multiple objectives. One notable study in the early 2000s, conducted by Papadrakakis *et al*. (2002), focused on multi-objective problems in framed structures under static and dynamic loading conditions. The study presented numerical examples applied on 3D frames and large-scale trusses, with objectives to minimize both weight and maximum displacement for framed structures, and to maximize the first natural frequency of vibration while minimizing weight for trusses. Another study by Kicinger and Arciszewski (2004) presented a multi-objective problem of frames with different bracing configurations for plane structures representing tall buildings. The study subjected the structures to an evolutionary optimization process with two conflicting objectives: minimizing the total weight of the structure and minimizing the maximum displacement. Subsequent research by Kicinger *et al*. (2007) investigated multi-objective optimization for frames with different bracing systems, utilizing the Strength-Pareto Evolutionary Algorithm II (SPEA2) in conjunction with a mathematical optimization method. In a related study, Liu *et al*. (2005) developed a methodology for earthquake-resistant civil structures that balances the minimization of two conflicting objective functions: short-term construction investment and long-term risk of earthquakes. The study proposed objective functions that incorporate material consumption, initial construction expenses, seismic structural performance, and lifetime cost of earthquake damage.

In the early 2010s, Yazdi *et al*. (2010) investigated the optimal geometric configuration of the three bars comprising an eccentric bracing system, focusing on the position of the connection point. The study had two conflicting objectives, namely minimizing weight and maximizing stiffness to lateral displacements, and utilized fuzzy logic to determine the best configuration. Elkassas and Swelem (2012c) conducted a case study of multi-story flat frames located in Egypt, considering three different types of bracing (type "A", type "V", and type "X") to find the most economical bracing system within allowable stress limits for wind loads. Richardson *et al*. (2013) sought to define an efficient bracing configuration for a museum in the United States through multi-objective optimization, studying the optimal distribution of "X" braces on the building's four facades. The study had two conflicting objectives, minimizing the cost of development and inter story drift.

In the mid-2010s, Kaveh and Farhoudi (2015) proposed a novel study that utilized Differential Evolution and Dolphin Echolocation algorithms as search methods to optimize the layout of plane

Table 1 Aspects of related works regarding design variables and number of simultaneous objectives considered

Year	Authors	Design Variables			NSO			
		BS	CO	S	1	2	3	4
2002	Papadrakakis *et al*.			OK		OK		
2004	Kicinger and Arciszewski	OK		OK		OK		
2005	Liu			OK		OK		
2007	Kicinger *et al*.	OK		OK		OK		
2010	Yazdi *et al*.			OK		OK		
2010	Kizilkan		OK	OK	OK			
2012	Elkassas and Swelem	OK		OK	OK			
2012	Lemonge and Barbosa		OK	OK	OK			
2013	Richardson *et al*.	OK		OK		OK		
2015	Kaveh and Farhoudi	OK		OK	OK			
2016	Babaei and Sanaei	OK		OK		OK		
2016	Gholizadeh and Poorhoseini	OK		OK	OK			
2017	Barraza *et al*.			OK		OK		
2017	Gholizadeh and Baghchevan			OK		OK		
2017	Hasanaçebi	OK		OK	OK			
2018	Kaveh *et al*.	OK		OK	OK			
2019	Braga *et al*.	OK		OK	OK			
2019	Khaledy *et al*.			OK		OK		
2019	Burton *et al*.			OK		OK		
2019	Baradaran and Madhkhan	OK		OK	OK			
2020	Farahmand-Tabar and Ashtari	OK		OK	OK			
2020	Tu *et al*.			OK		OK		
2020	Resende *et al*.			OK		OK		
2021	Do and Ohsaki			OK		OK		
2021	Ghasemof *et al*.			OK		OK		
2021	Gholizadeh and Fattahi			OK		OK		
2021	Motta *et al*.		OK	OK		OK		
2021	Shen *et al*.			OK		OK		
2023	This work	OK	OK	OK				OK

frames. The study aimed to identify the optimal bays for locating "X" bracing systems while minimizing the weight of the structure. Babaei and Sanaei (2016) focused on the cross-sections of beams and columns and topology changes in the bracing system as design variables. They utilized a multi-objective optimization algorithm to minimize weight and maximum displacement. Gholizadeh and Poorhoseini (2016) also applied the Dolphin Echolocation algorithm to minimize the cost of the bracing configuration. Two years later, Kaveh *et al*. (2018) c conducted a similar study but with different design variables and objective functions. Hasançebi (2017) proposed a cost-benefit analysis for economic steel frame designs, considering various bracing systems and beam-column connections for 13 different building models. These studies highlight the use of diverse optimization algorithms to solve structural optimization problems and obtain more practical cost-effective designs for steel frames.

Several recent studies have explored optimization methods for designing efficient and cost-effective bracing systems for steel frames. Braga *et al*. (2019) proposed a multi-performance optimization approach for designing dissipative bracing systems that minimize the cost of intervention. Khaledy *et al*. (2019) aimed to minimize the weight and damage index of plane steel frames subjected to explosion loads, while Burton *et al*. (2019) conducted a multi-objective optimization study of controlled rocking steel braced frames. Baradaran and Madhkhan (2019) evaluated different topologies for mega bracing systems, which are commonly used for lateral stiffening, and Farahmand-Tabar and Ashtari (2020) investigated inclined bracing trusses for tall buildings with out-rigger braced systems.

Numerous significant contributions in the field of truss analysis and optimization warrant attention. Tejani *et al*. (2017) employed a pedagogical and experiential learning strategy to explore the optimization of topology, shape, and size of truss structures. Noteworthy studies by Kaveh and Bakhshpoori (2016), Kaveh and Rezaei (2016), Kaveh and Ilchi Ghazaan (2016) encompassed the application of efficient multi-objective search algorithms for design optimization. These studies addressed truss optimization with dynamic constraints, topology optimization, and geometry optimization for various dome configurations. Turning to the domain of composite structures, Akbulut *et al*. (2020) conducted a meticulous examination utilizing non-linear optimization techniques to assess the performance of composite structures under conditions of vibration and buckling loads. This investigation contributes significantly to the evolving comprehension of composite structure optimization, shedding light on their behavior under critical loading scenarios. Finally, in the field of grid structures, Cascone *et al*. (2021) conducted an investigation into the optimization of diagrid structures applied in the context of tall buildings, while Tomei *et al*. (2022) focused their study on the design optimization of gridshells.

Table 1 compiles the cited works related to steel frames, as well as additional similar works and the current study to enable a comparative analysis of design variables and the number of objectives simultaneously considered, where BS is bracing system configuration, CO is column orientation, S is the cross-section, and NSO means number of simultaneous objectives considered. The present work stands out due to the unique approach of considering the bracing systems as a variable, the simultaneous consideration of design variables from three distinct categories, and the consideration of four objectives in the problem formulation.

3. Formulation of the multi-objective optimization problem

The multi-objective optimization problem aims to determine the best bracing system configuration, column orientations, and commercial steel profiles described by an integer index vector $x = \{I_1, I_2, ..., I_i\}$ (design variables) outlined in Subsection 5.3. These design variables should satisfy the problem objectives, which are: (i) minimizing the total weight of the structure $(W(x))$; (ii) minimizing the maximum horizontal displacement $(\delta_{max}(x))$; (iii) maximizing the first natural frequency of vibration $f_1(x)$; and (iv) maximizing the critical load factor for global stability $(\lambda_{crt}(x))$. Eq. (1) formalizes the multi-objective problem formulation, where x^L and x^U represent the lower and upper bounds of the design variables, respectively. The expression for the total weight of the structure is provided in Eq. (2) which involves the specific mass of the material denoted by ρ, and the cross-sectional area A_i and length L_i of the i-th element.

$$\begin{gathered}\min W(x)\ and\ \min \delta_{max}\ and \max f_1(x)\ and \max\ \lambda_{crt}(x)\\ \text{s.t. strucutural constraint } x^L \le x \le x^U\end{gathered} \tag{1}$$

$$W(x) = \sum_{i=1}^{N} \rho A_i L_i \tag{2}$$

3.1 Design constraints

The design constraints in the problems addressed in this paper can be divided into three groups: displacement constraints, strength constraints, and geometric constraints.

3.1.1 Displacement constraints

There are two constraints imposed on the structural displacements in the problems addressed in this paper. The first constraint concerns the maximum horizontal displacement at the top of the building ($\delta_{max}(x)$); and is defined by Eq. (3), where $\bar{\delta} = H/400$ represents the maximum allowable displacement. Here H, denotes the height of the structure. The second constraint is related to the inter-story drift of the i-th floor of the building $d_i(x)$ and is defined by Eq. (4) where $\bar{d} = h/500$ is the maximum allowable inter-story drift, h is the ceiling height, and N_s is the total number of stories (ABNT 2008).

$$\frac{\delta_{max}(x)}{\bar{\delta}} - 1 \le 0 \tag{3}$$

$$\frac{d_i(x)}{\bar{d}} - 1 \le 0 \quad i = 1, \dots, N_s \tag{4}$$

3.1.2 Strength constraints

The structural members are subject to Load and Resistance Factor Design (LRFD) equations (ANSI 2016), which encompass axial and unsymmetrical bending, as well as shearing effects. These equations are applicable to doubly symmetric cross-sectional members and adhere to the guidelines outlined in ANSI (2016) and Brazilian Codes for Steel Construction (ABNT 2008). The LRFD equations (Eqs. (5) and (6)) specify that the required axial strength, P_r, and the flexural strengths about the major and minor axis, M_{rx} and M_{ry}, must be satisfied by the available axial and flexural strengths, designated as P_c, M_{cx}, and M_{cy}. Similarly, the required and available shearing strengths are denoted as V_r and V_c, respectively. The available strengths are evaluated in accordance with Brazilian and American technical codes (ABNT 2008, ANSI 2016), accounting for the reduction in section effectiveness due to local and global buckling. The effective buckling length factor is taken as K=1.0, which is recommended in ABNT (2008) for multi-story braced frames.

$$\begin{cases} \dfrac{P_r}{P_c} + \dfrac{8}{9}\left(\dfrac{M_{rx}}{M_{cx}} + \dfrac{M_{ry}}{M_{cy}}\right) - 1 \le 0 & if\ \dfrac{P_r}{P_c} \ge 0.2 \\ \dfrac{P_r}{2P_c} + \left(\dfrac{M_{rx}}{M_{cx}} + \dfrac{M_{ry}}{M_{cy}}\right) - 1 \le 0 & if\ \dfrac{P_r}{P_c} \ge 0.2 \end{cases} \tag{5}$$

$$\frac{V_r}{V_c} - 1 \leq 0 \tag{6}$$

3.1.3 Geometric constraints

This formulation applies geometric constraints to the column-to-column fitting to prevent sections with greater depth or mass from being fitted over sections with lesser depth or mass. The constraints concerning the depth and mass of the sections are governed by Eqs. (7) and (8), respectively. Here, $dp_i(x)$ and $dp_{i-1}(x)$ represent the depth of the W section selected for the group of columns i and $i-1$, respectively, and $ms_i(x)$ and $ms_{i-1}(x)$ are the unit weight of the W section selected for the group of columns i and $i-1$, respectively. NG_c denotes the number of groups of columns.

$$\frac{dp_i(x)}{dp_{i-1}(x)} - 1 \leq 0 \qquad i = 1, \ldots, NG_c \tag{7}$$

$$\frac{ms_i(x)}{ms_{i-1}(x)} - 1 \leq 0 \qquad i = 1, \ldots, NG_c \tag{8}$$

4. Materials and methods

Multi-objective optimization is a common problem in which multiple objectives need to be considered simultaneously. The outcome of such a problem is a set of non-dominated solutions generating a PF. This front is essentially a trade-off curve, which displays the relationship between the different objectives and the corresponding solutions. By examining this curve, designers can extract solutions that meet their requirements while considering trade-offs between conflicting objectives. There are various methods available for extracting solutions from the PF, allowing designers to choose the most appropriate solution according to their preferences.

4.1 Dominance and optimal PF

To rank the solutions obtained in a multi-objective problem, the concept of dominance is employed. This approach is similar to the one introduced by Deb (2001). In a minimization problem, a solution A dominates another solution B $(A \prec B)$ if one of two conditions holds: either A is better or equal to B in all objective functions ($f_i(A) \leq f_i(B)$ for all $i = 1, 2, \ldots, n$, where n is the number of objectives), or A is strictly better than B in at least one objective function ($f_i(A) < f_i(B)$ for at least one value of i). Handling the constraints, feasible solutions are compared with non-feasible solutions using the NSGA-II ranking and crowding distance scheme (Deb *et al*., 2002). This approach allows for an efficient ranking of solutions, providing valuable insights for designers in selecting the most appropriate solution from the PF.

4.2 Evolutionary algorithms adopted

The algorithms employed in this study are all based on differential evolution. To conduct a more comprehensive analysis, four distinct algorithms are adopted, namely: (i) The Third

Evolution Step of Generalized Differential Evolution (GDE3) proposed by Kukkonen and Lampinen (2005); (ii) The Success History Based Adaptive Multi-objective Differential Evolution (SHAMODE) introduced by Panagant *et al*. (2019); (iii) The Success History Based Adaptive Multi-objective Differential Evolution with Whale Optimization (SHAMODE-WO), which incorporates the spiral movement from the Whale Optimization Algorithm (WOA) created by created by Mirjalili and Lewis (2016), also developed by Panagant *et al*. (2019); and (iv) The Multi-objective Meta-heuristic with Iterative Parameter Distribution Estimation (MMIPDE) proposed by Wansasueb *et al*. (2022). To determine the next set of candidate solutions for future generations, the concepts of dominance and crowding distance, as described by Deb *et al*. (2002), are used. This approach ensures a robust selection process, enabling the identification of high-quality solutions in a multi-objective optimization problem. The constraints are handled using the constraint-based non-dominated sorting technique described in Deb *et al*. (2002), or constraint dominance principles, in which for any two solutions x and y: (i) If x is feasible and y is infeasible x is ranked above y; (ii) If x and y are both infeasible the one with the smaller constraint violation is ranked higher; and (iii) If x and y are both feasible the one dominating the other is ranked higher.

4.3 Multi-criteria decision-making

Once the PF has been obtained, it is necessary for the designer to extract the most suitable solution for the design at hand. This can be achieved either by visually identifying the most appropriate solution on the trade-off curve or by adopting systematic extraction methods. In this paper, a multi-criteria decision-making method, as detailed by Parreiras and Vasconcelos (2009), is employed, whereby the importance of each objective is weighted to facilitate the automatic extraction of solutions. This approach enables a more informed and objective decision-making process and facilitates the identification of the most suitable solution to meet the design requirements.

The decision-making problem involves selecting a solution in a multi-objective problem, with a set of alternatives representing the Pareto front and weighted criteria. The MTD method uses tournaments and the function $R(a)$ to rank solutions based on criteria defined by the decision maker. The function $R(a)$ combines the weighted criteria, where w_i are the importance weights, and is defined based on tournament victories (Eqs. (9), (10) and (11)). The weights w_i are defined with the condition that $w_i \geq 0$ and the total sum equal to 1. The function $R(a)$ quantifies the preference of one solution over another: If $R(a) > R(b)$, a is preferred over b; If $R(a) = R(b)$, a is considered indifferent to b. Where m is the number of objective functions.

$$T_i(a, A) = \sum_{\forall b \in A, a \neq b} \frac{t_i(a, b)}{(|A| - 1)} \tag{9}$$

$$t_i(a, b) = \begin{cases} 1 & if \quad f_i(a) - f_i(b) > 0 \\ 0 & otherwise \end{cases} \tag{10}$$

$$R(a) = \left(\prod_{i=1}^{m} T_i(a, A)^{w_i} \right)^{1/m} \tag{11}$$

4.4 Performance evaluation

In order to conduct a comprehensive evaluation of algorithmic performance, two widely recognized and efficient performance metrics were employed: the Hypervolume (HV) and the Inverted Generational Distance Plus (IGD+). The Hypervolume metric, introduced by Zitzler and Thiele (1999), is a well-established measure in the field of multi-objective optimization. It quantifies the quality and spread of solutions achieved by an algorithm in the objective space. By calculating the volume covered by the Pareto front approximation, the Hypervolume metric provides valuable insights into the effectiveness of an algorithm in exploring and capturing the trade-off between multiple conflicting objectives. Additionally, the Inverted Generational Distance Plus (IGD+), proposed by Ishibuchi *et al*. (2015), is another performance metric employed in the evaluation process. The IGD+ metric evaluates the closeness of a set of obtained solutions to the true Pareto front. It considers both the coverage and proximity of the solutions, enabling a comprehensive assessment of an algorithm's ability to approximate the optimal front. This measure plays a crucial role in quantifying the convergence and diversity aspects of an algorithm's performance.

5. Numerical experiments

This paper presents the results of three structural multi-objective optimization experiments conducted on 3D frames of varying dimensions. The first experiment involved a four-story and four-bay frame, the second an 8-story and 6-bay frame, and the third a 12-story and 12-bay frame, each with a uniform story-height of three meters. Six different scenarios, with distinct preference weights, were used to extract the desired non-dominated solutions.

The first objective function considered is the total weight of the structure, the second is the maximum horizontal displacement, the third is the first natural frequency of vibration, and the fourth is the critical load factor concerning the first global buckling mode. The scenarios were defined with the following importance weights: [1 0 0 0], [0 1 0 0], [0 0 1 0], [0 0 0 1], [0.25 0.25 0.25 0.25], and [0.7 0.1 0.1 0.1]. Each of the scenarios was analyzed and detailed, and the resulting PFs were represented in parallel coordinates, as described by Li *et al*. (2017). In this work, the solutions were represented using a normalized parallel coordinates system, represented as a poly-line in the vector space of the normalized objective functions in the range from 0 to 1. To obtain these solutions, ten independent runs of 300 generations with 50 candidate vectors were conducted for the four algorithms employed. For the DE algorithm, the scale factor are considered to be $F = 0.4$ and the crossover probability $C_r = 0.9$.

5.1 General assumptions

This paper assumes that the orientation of columns will not impact the building's interior architecture. The structures under consideration are commercial buildings with inner partitions and glass facades. Furthermore, the search space for columns is limited to H-shaped profiles with depths that are nearly equal to the flange width. The seismic design is not considered in the optimization process, as it is not mandatory according to Brazilian codes (ABNT 2008) and at least two load combinations are taken into account in each structure, considering the wind pressure acting in two orthogonal directions. Lateral displacements are evaluated in these directions.

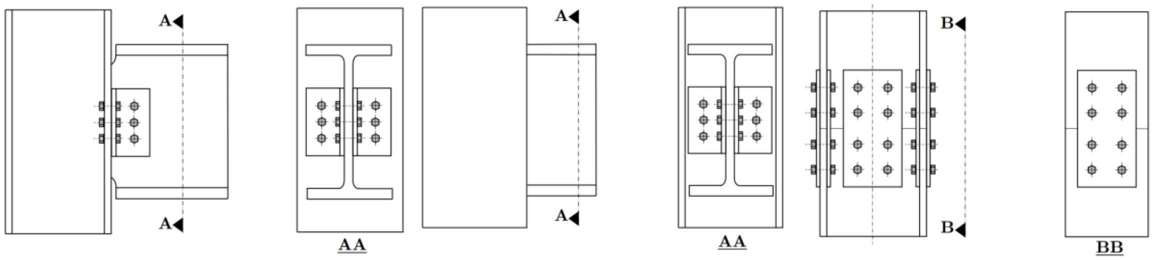

(a) Beam-to-column (Flexible) (b) Beam-to-column (Flexible) (c) Column-to-column (Rigid)

Fig. 1 Elements connections

A modelling technique based on the multi-freedom constraints approach, as detailed in Felippa (2004), is adopted to account for the effects of the slabs in the structure. This approach induces a rigid diaphragm behaviour of the floor plane, thus allowing for considering both the mass and stiffness of the slabs in determining the structure's displacements and frequencies. Specifically, the slabs' masses are treated as equivalent nodal masses in the evaluation of the first natural frequency of vibration. The slabs are considered to have a specific mass of 2400 kg/m^3 and 0.1 m of thickness. It is important to remark that the weight of the slabs is not added to the structure's weight in the optimization problem, as only the steel frames are considered.

All the structures in the experiments are braced spatial steel frames, so the beam-to-column connections are assumed to be pin-jointed; that is, only the web of the profile is attached to the column by two angle bars, as detailed in Fig 1(a)-(b).

All the beams are attached to the columns only by their section web, and as the bending moments near this kind of joints are minimal, it is not mandatory that the flange must be full in the connection. Thus, in cases where a beam's flange is wider than the column's web, the beam's flange may be bevelled or trimmed to fit properly into the connection. The columns are assumed to be rigidly connected by the flanges and the web (Fig. 1(c)). Also, the beams are considered to be laterally supported by the slab through shear studs, so there is no loss of effectiveness due to lateral torsional buckling.

5.2 Design loads

The design loads of the structure are divided into three types: dead loads (DL), live loads (LL), and wind loads (W). Dead loads refer to the self-weight of the steel structure and slabs, and the weight of its constructive elements, such as dividing walls, and glass facades. Live loads represent the weight imposed by the use and occupation of the structure, while wind loads are the forces generated by the dynamic pressure of the wind. For all experiments conducted in this paper, it is considered the steel frame self-weight, a slab dead load (DL_s =2.4 kN/m^2), an inner partition dead load acting on the inner beams (DL_{ip} =5.85 kN/m), a glass facade dead load acting on the outer beams (DL_{gf} = 0.6 kN/m), a live load (LL = 1.5 kN/m^2), and a set of nodal wind loads for each experiment evaluated according to ABNT (1988) for a basic velocity of 37 m/s. Two load combinations are verified for each experiment taking into account the wind direction, and these combinations are defined according to ABNT (2002) and ABNT (2008), and can be written as follows: $LC_1 = 1.4 * DL + 1.5 * LL + 1.4 * W_x$ and $LC_2 = 1.4 * DL + 1.5 * LL + 1.4 * W_y$, where W_x and W_y are the wind load acting on -x and -y directions, respectively. The specific gravity and wind loads for each experiment are detailed in their respective sections.

Table 2 Search space composed of two subsets of commercial profiles

W shapes for Columns				W shapes for Beams							
1	W 150x22.5	16	W 250x89	1	W 150x13	16	W 310x21	31	W 410x38.8	45	W 530x66
2	W 150x29.8	17	W 250x101	2	W 150x18	17	W 310x23.8	32	W 410x46.1	47	W 530x72
3	W 150x37.1	18	W 250x115	3	W 150x24	18	W 310x28.3	33	W 410x53	48	W 530x74
4	W 200x35.9	19	W 310x79	4	W 200x15	19	W 310x32.7	34	W 410x60	49	W 530x82
5	W 200x41.7	20	W 310x93	5	W 200x19.3	20	W 310x38.7	35	W 410x67	50	W 530x85
6	W 200x46.1	21	W 310x97	6	W 200x22.5	21	W 310x44.5	36	W 410x75	51	W 530x92
7	W 200x52	22	W 310x107	7	W 200x26.6	22	W 310x52	37	W 410x85	52	W 530x101
8	W 200x53	23	W 310x110	8	W 200x31.3	23	W 360x32.9	38	W 460x52	53	W 530x109
9	W 200x59	24	W 310x117	9	W 250x17.9	24	W 360x39	39	W 460x60	54	W 610x101
10	W 200x71	25	W 310x125	10	W 250x22.3	25	W 360x44	40	W 460x68	55	W 610x113
11	W 200x86	26	W 360x91	11	W 250x25.3	26	W 360x51	41	W 460x74	56	W 610x125
12	W 250x62	27	W 360x101	12	W 250x28.4	27	W 360x57.8	42	W 460x82		
13	W 250x73	28	W 360x110	13	W 250x32.7	28	W 360x64	43	W 460x89		
14	W 250x80	29	W 360x122	14	W 250x38.5	29	W 360x72	44	W 460x97		
15	W 250x85			15	W 250x44.8	30	W 360x79	45	W 460x106		

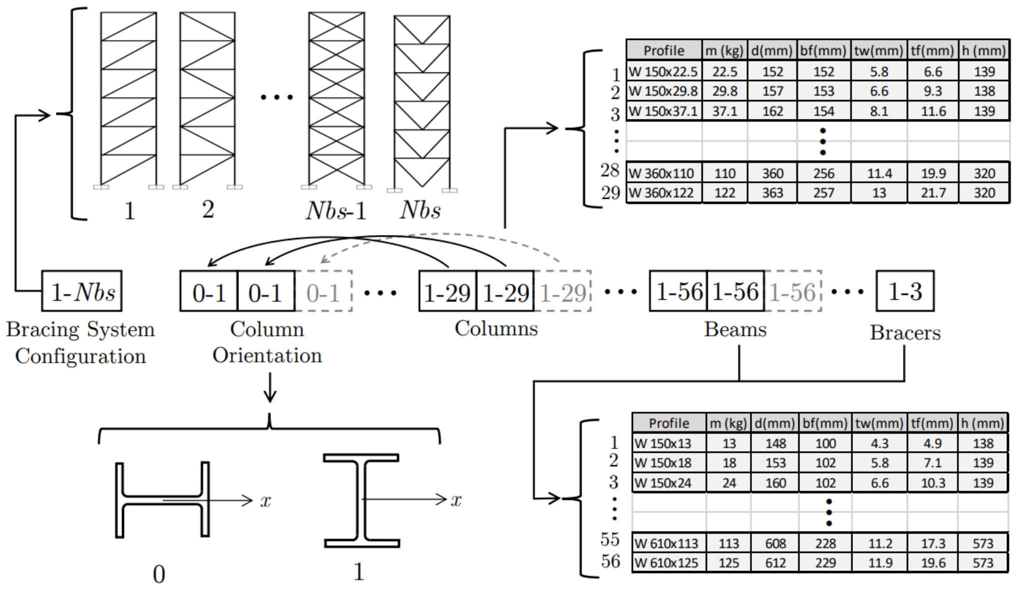

Fig. 2 Candidate vector for a general problem, including bracing system configuration, column orientation and commercial profiles variables

5.3 Design variables and search space

The candidate vector concerning the design variables is divided into five subsets of integer indexes. The first index is related to the bracing system configuration that will stiffen the structure, with a range of possible values from one to *Nbs*, in which *Nbs* is the number of available bracing

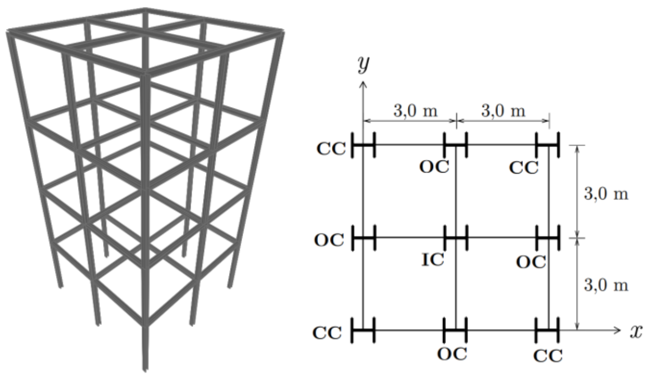

Fig. 3 Experiment 1 – 3D and plain view of the 4-story and 4-bay space frame

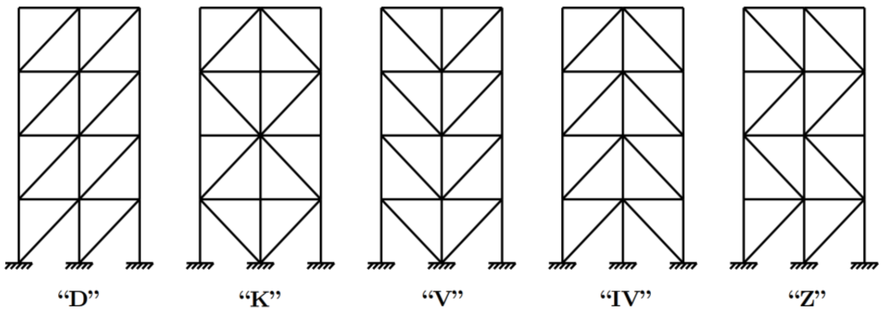

Fig. 4 Experiment 1 – Possible bracing systems configurations

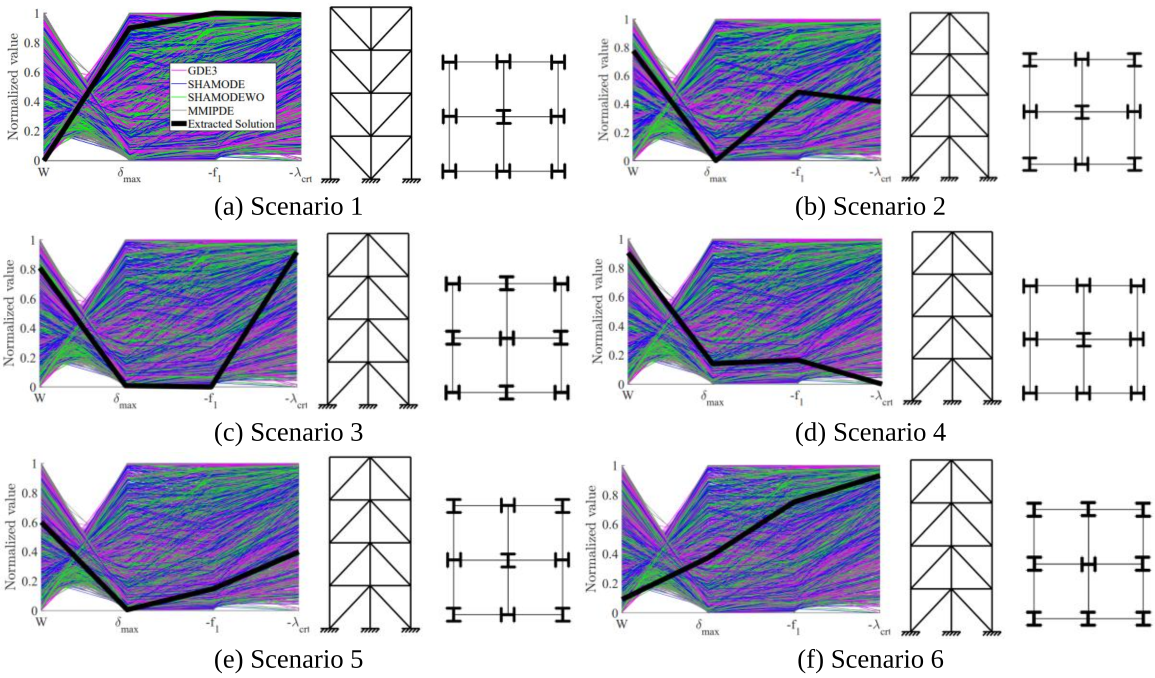

(a) Scenario 1

(b) Scenario 2

(c) Scenario 3

(d) Scenario 4

(e) Scenario 5

(f) Scenario 6

Fig. 5 Experiment 1 results: Parallel coordinates in the objective functions domain

Table 3 Experiment 1 – Wind loads acting on façade nodes

Story	Height (m)	Corner Nodes (kN)	Middle Nodes(kN)
1	3	3.19	6.39
2	6	3.34	6.67
3	9	3.68	7.35
4	12	1.97	3.94

Table 4 Experiment 1 – Best results found for the six extracted scenarios, presenting details of the profiles assigned to each member group, constraints, and objective functions

Scenario	1	2	3	4	5	6
Importance weights	[1 0 0 0]	[0 1 0 0]	[0 0 1 0]	[0 0 0 1]	[0.25 0.25 0.25 0.25]	[0.7 0.1 0.1 0.1]
Bracing System	**V**	**IV**	**IV**	**IV**	**IV**	**IV**
Group (Stories)	W Profiles					
CC (1-2)	150x22.5	310x125	360x122	360x122	310x125	150X22.5
CC (3-4)	150x22.5	310x125	150X22.5	200x71	150X37.1	150X22.5
OC (1-2)	150x22.5	360x122	360x122	310x125	360x101	150X22.5
OC (3-4)	150x22.5	360x122	150x22.5	310x125	200X52	150X22.5
IC (1-2)	150x22.5	360x122	360x122	310X117	310X117	310x79
IC (3-4)	150x22.5	360x110	150x22.5	310X97	310X93	310x79
OB (1-2)	150x13	530X101	610X125	610X125	360X72	150X13
OB (3-4)	150x13	530X74	610X125	610X125	610X113	200X26.6
IB (1-2)	250x17.9	610x101	610X125	610X125	460X60	150X24
IB (3-4)	250x17.9	360X32.9	610X125	530X101	200X31.3	250X32.7
BC (1-4)	150x13	150x24	150x24	150x18	150x24	150x18
Constraints and objective functions values						
LRFD (x)	0.85	0.31	0.47	0.12	0.49	0.85
V_{max} (x)	0.19	0.11	0.03	0.04	0.17	0.22
d_{max} (x) (mm)	0.5	0.2	0.2	0.3	0.2	0.3
δ_{max} (x) (mm)	1.8	0.6	0.6	0.8	0.6	1.1
f_1 (Hz)	1.61	4.18	6.61	5.78	5.87	2.85
λ_{crt}	3.69	58.41	10.59	98.22	60.04	9.28
W(x) (kg)	6349	28323	29242	31944	23331	8922
Search method						
Algorithm	GDE3	GDE3	GDE3	GDE3	MMIPDE	SHAMODE-WO

system configurations in the problem. The second subset of indexes determines the orientation of the cross-section of the columns, which is a binary choice indicating the position of the highest and lowest principal moment of inertia concerning the global x-axis of the structure. The third subset of variables corresponds to the W-shaped commercial profiles assigned to the columns. Depending on the numerical experiment, each index is assigned to a group of elements, such as corner columns, outer columns, and inner columns. Each group of columns is linked to an orientation from the previous subset. The last two subsets of variables are related to the commercial profiles assigned to the beams and bracer elements. The search space for these subsets comprises 29 profiles for the columns and 56 profiles for the beams, as detailed in Table 2. The candidate vector is detailed in Fig. 2.

5.4 Experiment 1 (F4_4)

The first numerical experiment involves the multi-objective optimization of a 3D frame consisting of four stories and four bays, as shown in Fig. 3. The frame has columns that are divided into three groups: corner columns (CC), outer columns (OC), and inner columns (IC). Each group is assigned a profile repeated every two stories, resulting in six column variables. The beams are divided into outer beams (OB) and inner beams (IB) and, like the columns, are assigned the same profile every two stories, giving a total of four beam groups. The bracing system configurations are illustrated in Fig. 4. The gravity load acting on the beams is 16.60 kN/m for the inner beams and 5.05 kN/m for the outer beams, from the load combinations. Table 3 details the nodal wind loads. The results of the six extracted scenarios are presented in Table 4 and visualized in Fig. 5.

Six solutions were extracted and analyzed in this experiment. The first four scenarios are solutions that exhibit the best values for each of the objective functions, where one of the functions is given a weight of 1.0 of importance, and the others are given a weight of zero. The fifth scenario represents an intermediate solution, with equal weights assigned to each of the objective functions. The sixth scenario gives 0.7 importance to the structure's weight and 0.1 to the rest of the objective functions.

The solutions that exhibit the best objective function values are as follows: (i) scenario 1, with a weight of $W(x) = 6349$ kg; (ii) scenario 2, with a maximum horizontal displacement at the top of $\delta_{max}(x) = 0.6$ mm; (iii) scenario 3, with a first natural frequency of vibration of $f_1(x) = 6.61$ Hz; and (iv) scenario 4, with a critical load factor relative to global stability of $\lambda_{crt}(x) = 98.22$. It is noteworthy that the IV bracing system appeared in most of the extracted solutions, except for the lightest structure (scenario 1), which employed the V bracing system. Based on the results, it can be concluded that for this specific structure, the IV bracing system provides the best performance in terms of maximum horizontal displacement, the natural frequency of vibration, and global stability, while the V bracing system yields the lightest structure. It is important to remember that the solutions are obtained by a combination of variables, including the bracing system configuration, the orientation of the columns, and the profiles assigned to the members.

In the first four solutions, the orientation of the columns can be observed as follows: scenario 1 [0,0,1], scenario 2 [1,0,1], scenario 3 [0,1,0], and scenario 4 [1,1,0], with the ones and zeros according to Fig. 2. An interesting issue that can be observed in this experiment, more specifically in scenario 3, is that the maximization of the first natural frequency of vibration and the critical load factor is not redundant objectives, although both depend on the stiffness matrix of the structure. What is noticed is that the solution that leads to the highest vibration frequency of the PF (scenario 3, $f_1(x) = 6.61$ Hz, $\lambda_{crt}(x) = 10.59$), presents a factor of critical load well below the solution that presents the highest of all (scenario 4, $f_1(x) = 5.77$ Hz, $\lambda_{crt}(x) = 98.22$).

5.5 Experiment 2 (F8_6)

The second experiment conducted in this study involved an 8-story and 6-bay 3D frame, as

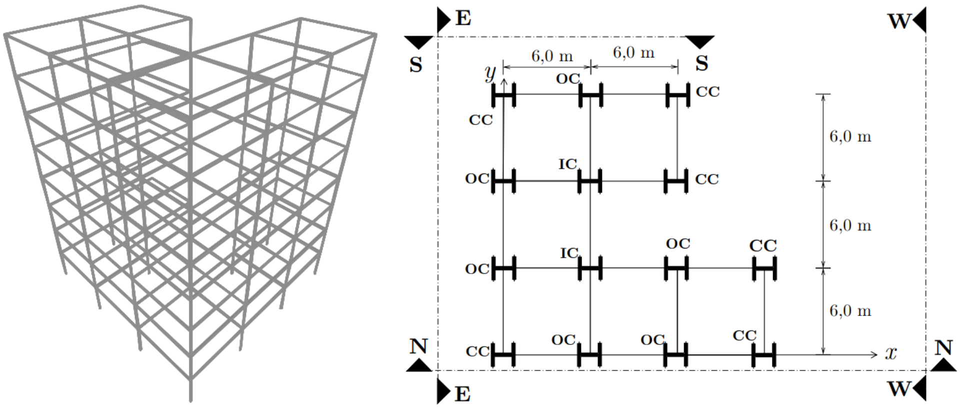

Fig. 6 Experiment 2 – 3D and plain view of the 8-story and 4-bay frame

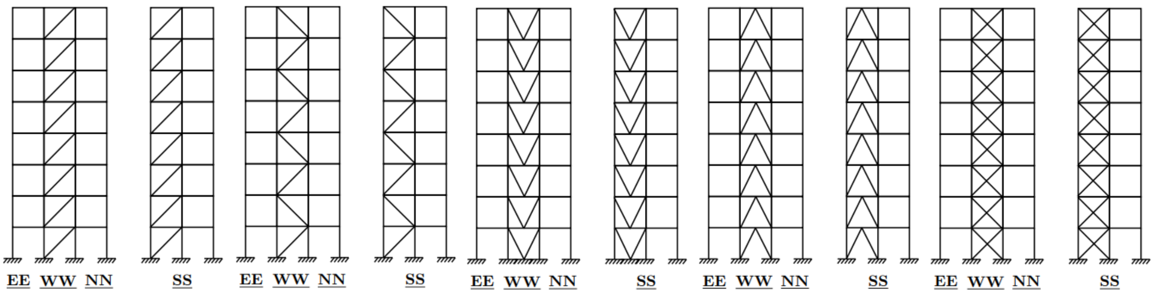

Fig. 7 – Experiment 1 – Possible bracing systems configurations. From left to right, Diagonal, "Z", "V", inverted V ("IV") and "X" geometric configurations

Table 5 – Experiment 2 – Wind loads acting on façade nodes

Story	Height (m)	Corner Nodes (kN)	Middle Nodes(kN)
1	3	3.79	7.58
2	6	3.95	8.30
3	9	4.36	8.72
4	12	4.67	9.34
5	15	4.93	9.86
6	18	5.14	10.28
7	21	5.34	10.68
8	24	2.76	5.51

depicted in Fig. 6. The frame was designed with column groups that were labeled for ease of reference. The experiment aimed to investigate five different bracing systems, which are shown in Fig. 7. The layout of the columns and beams was such that each column group and beam division repeated every four stories. Specifically, the beams were divided into outer beams and inner beams, just as in the first experiment. The load combinations used in this experiment included a gravity load acting on the beams. The gravity load was 25.02 kN/m for the inner beams and 9.25

Table 6 Experiment 2 – Best results found for the six extracted scenarios, presenting details of the profiles assigned to each member group, constraints, and objective functions

Scenario	1	2	3	4	5	6
Importance weights	[1 0 0 0]	[0 1 0 0]	[0 0 1 0]	[0 0 0 1]	[0.25 0.25 0.25 0.25]	[0.7 0.1 0.1 0.1]
Bracing System	**IV**	**X**	**X**	**V**	**X**	**X**
Group (Stories)	W Profiles					
CC (1-4)	250x62	360X122	360x122	360X122	360X122	360X91
CC (5-8)	200x35.9	200X46.1	200X35.9	360X122	310X97	150X22.5
OC (1-4)	310X97	360x122	360x122	310X125	310X125	150X22.5
OC (5-8)	200X59	310X93	150x22.5	310X110	310X93	150X22.5
IC (1-4)	360x122	310X125	360x122	360X122	360X122	310x79
IC (5-8)	360X91	310X125	360X122	360X122	310X117	310x79
OB (1-4)	250x17.9	460X106	610X125	610X125	360X44	250X17.9
OB (5-8)	250x17.9	530X92	610X125	610X125	360X72	200X26.6
IB (1-4)	410x38.8	530X101	610X125	610X125	460X82	360X57.8
IB (5-8)	410x38.8	610X125	610X125	610X125	610X101	310X52
BC (1-8)	150x18	150x24	150x24	150x24	150x24	150x18
Constraints and objective functions values						
LRFD (x)	0.98	0.55	0.66	0.61	0.57	0.97
V_{max} (x)	0.18	0.08	0.06	0.06	0.10	0.19
d_{max} (x) (mm)	1.9	1.1	1.1	1.3	1.1	1.5
δ_{max} (x) (mm)	15.0	8.0	8.2	10.5	8.1	10.1
f_1 (Hz)	0.36	0.79	0.85	0.82	0.77	0.54
λ_{crt}	1.02	4.49	3.74	7.59	5.99	2.79
W(x) (kg)	44633	138191	152864	161696	109291	61665
Search method						
Algorithm	SHAMODE -WO	SHAMODE -WO	GDE3	GDE3	SHAMODE -WO	MMIPDE

Table 7 – Experiment 3 – Wind loads acting on façade nodes

Story	Height (m)	C.Nodes(kN)	M.Nodes(kN)	Story	Height (m)	C.Nodes(kN)	M.Nodes(kN)
1	3	3.15	6.30	7	21	4.45	8.90
2	6	3.29	6.58	8	24	4.59	9.18
3	9	3.63	7.26	9	27	4.73	9.46
4	12	3.89	7.78	10	30	4.85	9.70
5	15	4.11	8.22	11	33	4.96	9.92
6	18	4.29	8.58	12	36	2.53	5.06

kN/m for the outer beams. In addition to the gravity load, nodal wind loads were also applied to the structure. Table 5 details the nodal wind loads. The results of the experiment were analyzed

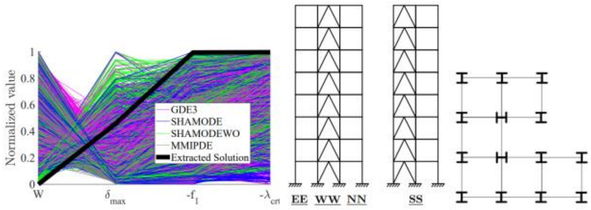

(a) Scenario 1

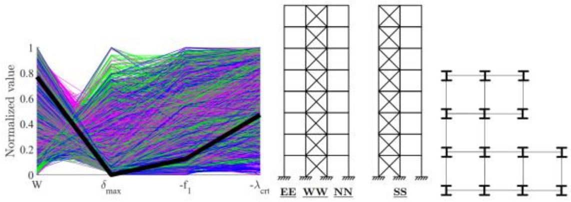

(b) Scenario 2

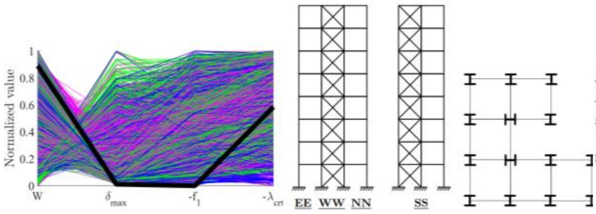

(c) Scenario 3

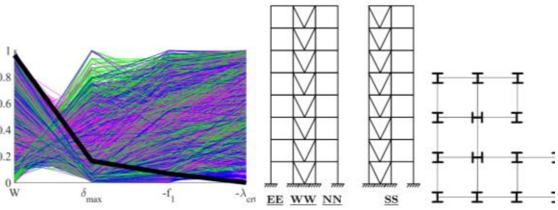

(d) Scenario 4

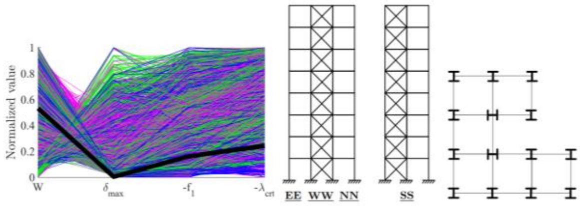

(e) Scenario 5

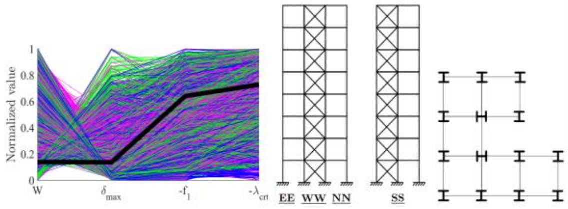

(f) Scenario 6

Fig. 8 Experiment 2 results: Parallel coordinates in the objective functions domain

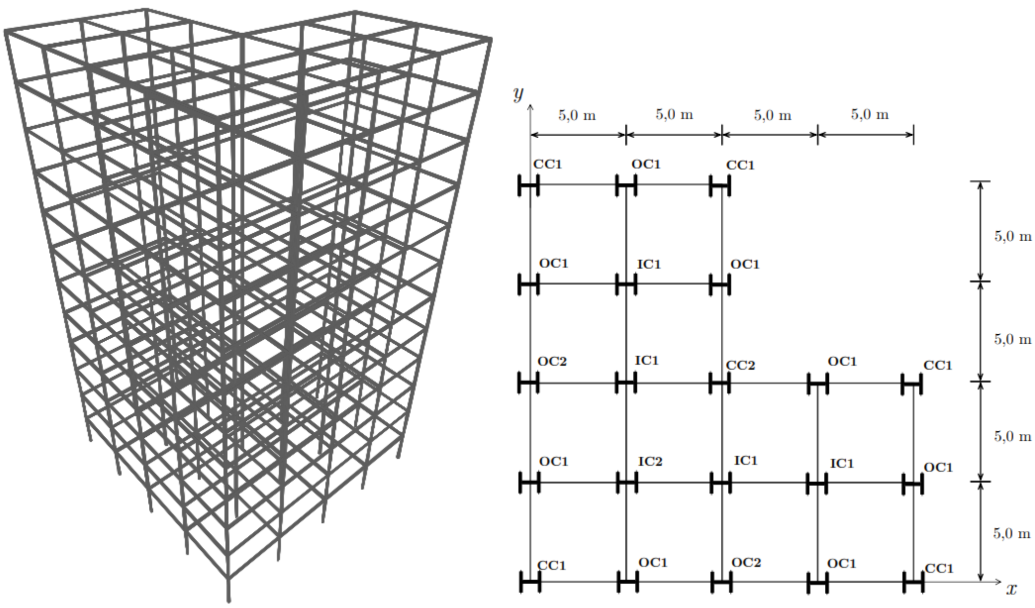

Fig. 9 Experiment 3 – 3D and plain view of the 12-story and 12-bay frame

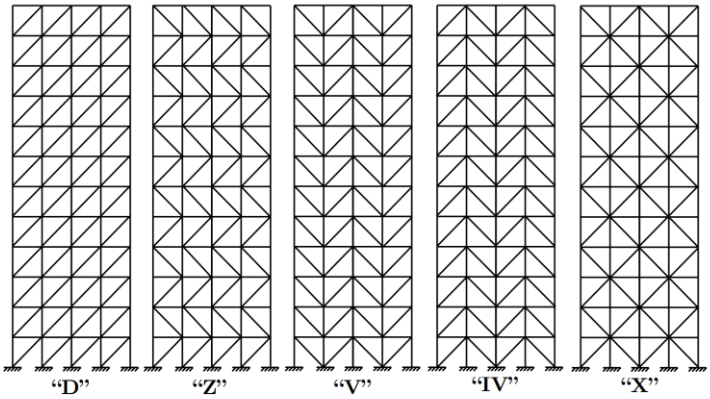

Fig. 10 Experiment 3 possible bracing systems configurations

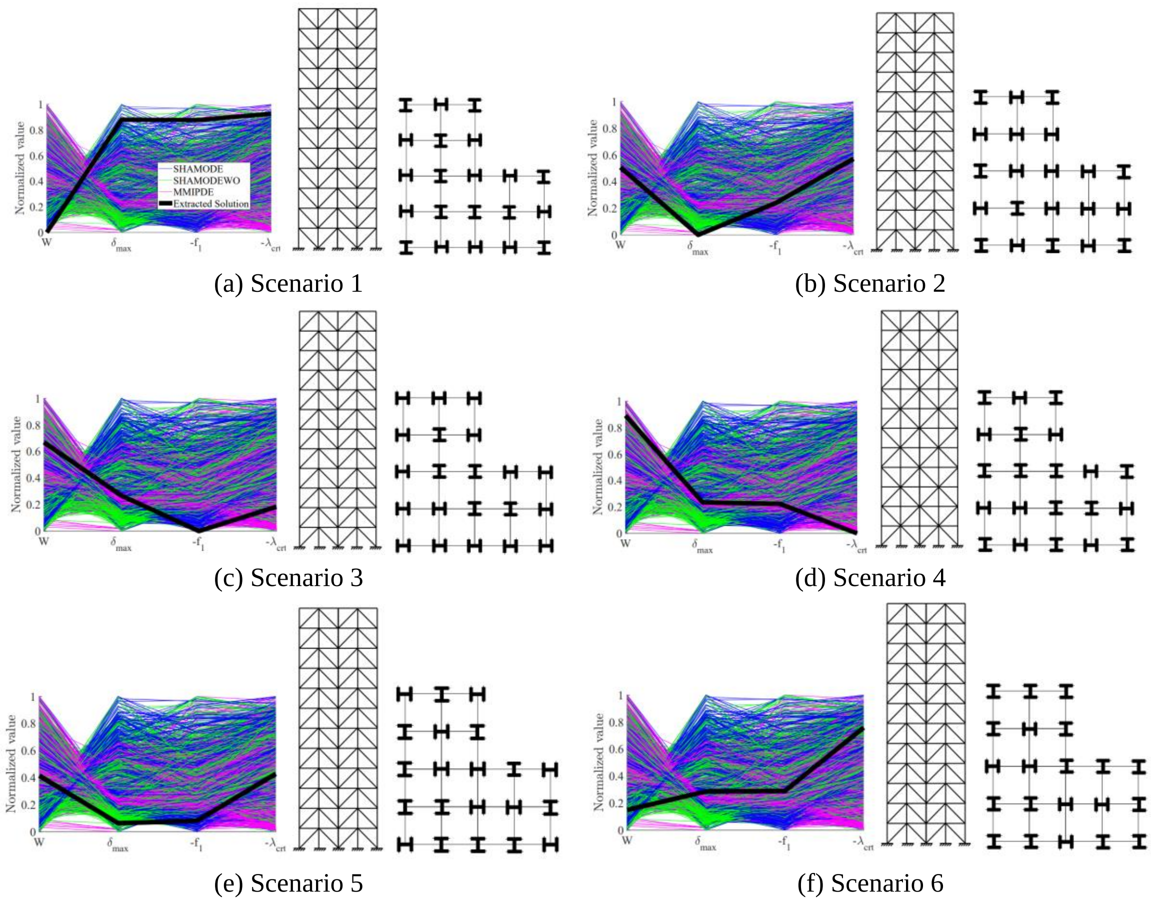

(a) Scenario 1 (b) Scenario 2

(c) Scenario 3 (d) Scenario 4

(e) Scenario 5 (f) Scenario 6

Fig. 11 Experiment 3 results: Parallel coordinates in the objective functions domain

through six different scenarios, and the outcomes are presented in Table 6. The results are also illustrated in Fig. 8.

Table 8 Experiment 3 – Best results found for the six extracted scenarios, presenting details of the profiles assigned to each member group, constraints, and objective functions

Scenario	1	2	3	4	5	6
Importance weights	[1 0 0 0]	[0 1 0 0]	[0 0 1 0]	[0 0 0 1]	[0.25 0.25 0.25 0.25]	[0.7 0.1 0.1 0.1]
Bracing System	**IV**	**X**	**X**	**V**	**X**	**X**
Group (Stories)	W Profiles					
CC1 (1-4)	360x91	360X122	310x117	360X122	360X122	310x117
CC1 (5-8)	200x41.7	250x115	310x117	360X122	360X122	310x117
CC1 (9-12)	150x22.5	150x37.1	150x37.1	310X110	150x22.5	150X22.5
CC2 (1-4)	310x110	200x41.7	310x125	360x91	360x91	310x117
CC2 (5-8)	200x52	200x35.9	310x107	250x89	250x73	310x117
CC2 (9-12)	150x37.1	200x35.9	200x46.1	200x86	200x59	310x117
OC1 (1-4)	360x91	360X91	310x117	310x117	310x117	310x107
OC1 (5-8)	310x125	200X52	310x79	310x117	250x62	150X22.5
OC1 (9-12)	200x35.9	150x22.5	150x29.8	250x80	150x37.1	150X22.5
OC2 (1-4)	310x125	310x79	360x122	360x122	200x35.9	310x117
OC2 (5-8)	250x80	200x52	200x71	360X122	150x29.8	200x71
OC2 (9-12)	200x41.7	150x29.8	200x46.1	310x97	150x22.5	200x41.7
IC1 (1-4)	310x125	310x117	360x122	360X122	360X122	310x117
IC1 (5-8)	310x107	310x107	310x107	360X122	310X93	310x117
IC1 (9-12)	200x71	250x73	250x73	360x101	250x73	250x73
IC2 (1-4)	310x28.3	310X117	310x117	360x122	360X110	310x125
IC2 (5-8)	310x107	310X79	310x117	360X122	360X110	310x117
IC2 (9-12)	200x71	200x52	310x117	310x107	360X110	310x110
OB (1-4)	310x28.3	360x79	610X125	610X125	530x101	460x60
OB (5-8)	250x17.9	610x125	610X125	610X125	530x72	200X26.6
OB (9-12)	250x25.3	360x79	610X101	610X125	530x82	250x32.7
IB (1-4)	360x32.9	460x97	530X109	610X125	360x57.8	250x38.5
IB (5-8)	310x38.7	360x72	360x64	610X125	360x72	310X44.5
IB (9-12)	360x32.9	360x57.8	360x64	530x66	310x44.5	310X38.7
BC (1-12)	150x18	150x24	150x24	150x24	150x24	150x24
Constraints and objective functions values						
$LRFD$	0.94	0.94	0.94	0.93	0.97	0.95
V	0.23	0.14	0.15	0.09	0.20	0.23
d (mm)	1.3	0.8	0.9	0.9	0.8	0.9
δ (mm)	10.5	4.1	6.0	5.8	4.5	6.2
f (Hz)	1.05	1.48	1.64	1.49	1.59	1.45
λ	1.46	3.39	5.51	6.51	4.17	2.37
W (kg)	130087	245796	282805	333495	224634	164251
Search method						
Algorithm	SHAMODE	SHAMODE	MMIPDE	MMIPDE	SHAMODE	MMIPDE

From Table 6 and examining the first four scenarios, it can be observed that the lightest solution has a weight of $W(x) = 44633$ kg. Meanwhile, the solution with the smallest maximum lateral displacement has a value of $\delta_{max}(x) = 8$ mm. In addition, the solution with the highest natural frequency of vibration has a value of $f_1 = 0.85$ Hz, and the solution with the highest critical load factor has a value of $\lambda_{crt}(x) = 7.59$. Regarding the bracing systems, it is worth noting that the IV configuration leads to the lightest structure. In contrast, the V configuration results in a structure with greater stability. The X configuration leads to structures that exhibit less horizontal displacement and a higher natural frequency of vibration. In scenario 3, it is observed that a similar phenomenon to that which occurred in experiment 1 takes place. Specifically, the solution that provides the highest vibration frequency (scenario 3, $f_1(x) = 0.85$ Hz, $\lambda_{crt}(x) = 3.74$) has a significantly lower critical load factor than the structure that exhibits greater stability (scenario 4, $f_1(x) = 0.82$ Hz, $\lambda_{crt}(x) = 7.59$), despite the orientation of the columns being the same in both scenarios [1,1,0] the bracing system configurations are different.

5.6 Experiment 3 (F12_12)

The third multi-objective optimization problem was solved for a 12-story, 12-bay 3D frame, as shown in Fig. 9. It is noteworthy that the groups of columns repeat every four stories. The load combinations acting on the beams include a gravity load of 22.21 kN/m for the inner beams and 7.85 kN/m for the outer beams. Table 7 provides the nodal wind loads. The results of the six scenarios that were analyzed are summarized in Table 8 and illustrated in Figure 11. Owing to the inherent difficulty of the GDE3 algorithm in generating feasible solutions despite an extensive number of generations, it was deemed unsuitable for inclusion in Experiment 3. As such, the remaining three algorithms were exclusively employed in the experiment.

The results obtained from the optimization process are significant and provide valuable insights into the design of efficient and stable structures. The findings show that for scenario 1, the structure's weight can be minimized to $W(x) = 130087$ kg, making it the lightest possible solution in the PF. Scenario 2 reveals that the available solution with a minimum horizontal deflection at the rooftop presents $\delta_{max}(x) = 4.1$ mm. Scenario 3 highlights that by carefully selecting the design parameters, the first natural frequency of vibration can be maximized to $f_1(x) = 1.64$ Hz. Finally, scenario 4 demonstrates that the critical buckling load can be optimized to $\lambda_{crt}(x) = 6.51$. Moreover, the findings indicate that the V configuration provides the lightest solution, making it a suitable option for scenarios where weight is a critical factor. The X configuration leads to the most stable structure, essential for structures exposed to severe loads. Lastly, the IV configuration is recommended for structures that require high resistance to horizontal displacement and maximum first natural frequency of vibration.

5.7 Performance indicators

In order to evaluate and compare the performances of the employed algorithms, two performance indicators, namely Hypervolume (HV) and Inverted Generational Distance Plus (IGD+), were utilized. The mean values and standard deviations for the three conducted experiments are presented in detail in 9. It is important to emphasize that, in the case of HV, a higher value indicates superior performance, whereas, for IGD+, the opposite holds true. The best values are highlighted in boldface in Table 9.

Significantly, it is noteworthy that despite GDE3 failing to find feasible solutions in

Table 9 – Performance Indicators

	GDE3		SHAMODE		SHAMODE-WO		MMIPDE	
	Mean	Std	Mean	Std	Mean	Std	Mean	Std
Experiment				HV				
(1)F4_4	0.347571	0.007116	0.335663	0.017412	0.324874	0.013167	0.336445	0.01435
(2)F8_6	0.428581	0.016355	0.412279	0.022078	0.41149	0.01926	0.419627	0.0152
(3)F12_12			0.424367	0.022743	0.423557	0.01984	0.431925	0.015645
				IGD+				
(1)F4_4	0.075529	0.008129	0.049321	0.007051	0.053246	0.005721	0.055224	0.006252
(2)F8_6	0.074538	0.011098	0.059882	0.012314	0.060394	0.007258	0.062036	0.00536
(3)F12_12			0.085687	0.021952	0.09045	0.023273	0.102182	0.044756

Experiment 3, it achieved the best performance in Experiments 1 and 2, as observed through HV analysis. On the other hand, MMIPDE presented the best performance in Experiment 3. Regarding IGD+, SHAMODE emerged as the algorithm with the best performance among all experiments. Consequently, various algorithms played a crucial role in addressing the problems investigated in this study, as no single algorithm exhibited clear superiority among the others. This conclusion is further reinforced upon analyzing the extracted solutions, which displayed considerable variability compared to the source algorithm. Even SHAMODE-WO, although it was not the optimal choice in any of the cases, achieved highly competitive values closely approaching those achieved by the best-performed algorithms. Importantly, it should be noted that the aforementioned analysis is contingent upon the specific optimization problem being addressed and is therefore limited to the numerical experiments conducted within the scope of this research.

6. Conclusions

This study presented a well-defined approach to tackle the complex multi-objective optimization problems of spatial steel frames. To achieve this, four different evolutionary algorithms based on differential evolution were adopted, in addition to a multi-criteria decision-making methodology to extract solutions from the PFs. This work provides novel contributions to the domain, especially in considering four objectives and effectively managing several design variables, including bracing system configuration, column orientation, and steel profiles obtained from commercial tables. Furthermore, the study conducted three numerical experiments, each encompassing six scenarios for thorough analysis.

Upon analysis, each algorithm demonstrated strengths and weaknesses. GDE3 performed best in Experiments 1 and 2, based on HV analysis, despite failing in Experiment 3. In contrast, MMIPDE excelled in Experiment 3. Notably, SHAMODE had the best overall performance in all experiments according to the IGD+ analysis. Extracted solutions showed variability compared to the source algorithm, and SHAMODE-WO, while not optimal in any case, displayed competitive values close to the best-performing algorithms.

Based on the analysis of the outcomes, it can be deduced that both the configuration of the optimal bracing system and the set of column orientations rely on the structure and the specific objectives under consideration, making it a challenging task to arrive at a solution based solely on the designer's expertise. Furthermore, solving an optimization problem with several objectives and generating a set of feasible solutions to be extracted according to the demands is a beneficial approach to implement during the initial sizing of large-scale projects. This method enables accurate estimation of the cost of the structure and its performance parameters, which, in this study, included horizontal displacements, dynamic behavior, and global stability. By addressing this problem, the designer gains valuable insights into the bracing system and the combination of profile section orientations that yield the most economical and efficient structures concerning performance.

As future works, this study can be extended to taller buildings and consider the $P-\delta$ and $P-\Delta$ effects in the calculation of solicitations and displacements within the evolutionary process. Additionally, considering more load combinations can further optimize the structure and bring it closer to the final design. These improvements will enhance the effectiveness of the optimization process and provide more accurate results for detailed design. Another potential area for development is the exploration of alternative optimization objectives that can balance the use of different profiles and weight reduction. Such an investigation can enable the designer to trade-off a lighter structure with fewer profiles, achieving savings in other aspects. Moreover, this approach could provide valuable information regarding the bracing system, column orientation, and profile grouping in an automated manner

Acknowledgments

This study was financed in part by the Coordenação de Aperfeiçoamento de Pessoal de Nível Superior – Brazil (CAPES) – Finance Code 001, and Conselho Nacional de Desenvolvimento Científico e Tecnológico (Grants 308105/2021-4 and 303221/2022-4), and FAPEMIG (Grants TEC PPM-00174-18 and APQ-00869-22).

References

ABNT (1988), *NBR 6123: Forças devidas ao vento em edificações*, ABNT Editora, Rio de Janeiro, Brasil.

ABNT (2002), *NBR 8681: Ações e segurança nas estruturas – Procedimento*, ABNT Editora, Rio de Janeiro, Brasil.

ABNT (2008), *NBR 8800: Projeto de estruturas de aço e de estruturas mistas de aço e concreto de edifícios*, ABNT Editora, Rio de Janeiro, Brasil.

Akbulut, M., Sarac, A. and Ertas, A.H. (2020), "An investigation of non-linear optimization methods on composite structures under vibration and buckling loads", *Adv. Comput. Des.*, **5**(3), 209-231. https://doi.org/10.12989/acd.2017.2.4.313.

ANSI (2016), \textit{AISC 360-16 Specification for Structural Steel Buildings}, AISC, Chicago, U.S.A.

Babaei, M. and Sanaei, E. (2016), "Multi-objective optimal design of braced frames using hybrid genetic and ant colony optimization", *Front. Struct. Civil Eng.*, **10**(4), 472-480. https://doi.org/10.1007/s11709-016-0368-4.

Baradaran, M. and Madhkhan, M. (2019), "Determination of optimal configuration for mega bracing systems in steel frames using genetic algorithm", *KSCE J. Civil Eng.*, **23**(8), 3616-3627. https://doi.org/10.1007/s12205-019-2369-z.

Barraza, M., Bojórquez, E., Fernández-González, E. and Reyes-Salazar, A. (2017), "Multi-objective optimization of structural steel buildings under earthquake loads using nsga-ii and pso", *KSCE J. Civil Eng.*, **21**(2), 488-500. https://doi.orh/10.1007/s12205-017-1488-7.

Braga, F., Gigliotti, R. and Laguardia, R. (2019), "Intervention cost optimization of bracing systems with multiperformance criteria'", *Eng. Struct.*, **182**, 185-197. https://doi.org/10.1016/j.engstruct.2018.12.034.
Burton, H.V., Lee, J.Y., Moradi, S. and Dastmalchi, S. (2019), "Multi-objective performance-based design optimization of a controlled rocking steel braced frame system", *Resil. Struct. Infrastruct.*, 243-268.
Carvalho, J., Carvalho, E., Vargas, D., Hallak, P., Lima, B. and Lemonge, A. (2021), "Multi-objective optimum design of truss structures using differential evolution algorithms", *Comput. Struct.*, **252**, 106544. https://doi.org/10.1016/j.compstruc.2021.106544.
Cascone, F., Faiella, D., Tomei, V., Lima, B. and Mele, E. (2021), "A structural grammar approach for the generative design of diagrid-like structures", *Buildings*, **11**(3), 90. https://doi.org/10.3390/buildings11030090.
Deb, K. (2001), *Multi-objective Optimization using Evolutionary Algorithms*, John Wiley & Sons, Kanpur, UP, India.
Deb, K., Pratap, A., Agarwal, S. and Meyarivan, T. (2002), "A fast and elitist multiobjective genetic algorithm: NSGA-II", *IEEE T. Evolution. Comput.*, **6**(2), 182-197. https://doi.org/10.1109/4235.996017.
Do, B. and Ohsaki, M. (2021), "Gaussian mixture model for robust design optimization of planar steel frames", *Struct. Multidiscipl. Opt.*, **63**(1), 137-160. https://doi.org/10.1007/s00158-020-02676-3.
Elkassas, E. and Swelem, S. (2012), "Optimization of bracing systems using neural networks", *Proceedings of the Eighth International Conference on Engineering Computational Technology*, Labuan, August.
Farahmand-Tabar, S. and Ashtari, P. (2020), "Simultaneous size and topology optimization of 3d outrigger-braced tall buildings with inclined belt truss using genetic algorithm", *Struct. Des. Tall Special Build.*, **29**(13). https://doi.org/10.1002/tal.1776.
Felippa, C.A. (2004), *Introduction to Finite Element Methods*, University of Colorado, Boulder, CO, U.S.A.
Ghasemof, A., Mirtaheri, M. and Mohammadi, R.K. (2021), "A new swift algorithm for bi-objective optimum design of steel moment frames'", *J. Build. Eng.*, **39**, 102162. https://doi.org/10.1016/j.jobe.2021.102162.
Gholizadeh, S. and Fattahi, F. (2021), "Multi-objective design optimization of steel moment frames considering seismic collapse safety", *Eng. Comput.*, **37**(2), 1315-1328. https://doi.org/10.1007/s00366-019-00886-y.
Gholizadeh, S. and Poorhoseini, H. (2016), "Seismic layout optimization of steel braced frames by an improved dolphin echolocation algorithm", *Struct. Multidiscipl. Opt.*, **54**(4), 1011-1029. https://doi.org/10.1007/s00158-016-1461-y.
Gholizadeh, S. and Baghchevan, A. (2017), "Multi-objective seismic design optimization of steel frames by a chaotic meta-heuristic algorithm", *Eng. Comput.*, **33**(4), 1045-1060. https://doi.org/10.1007/s00366-017-0515-0.
Hasançebi, O. (2017), "Cost efficiency analyses of steel frameworks for economical design of multi-storey buildings", *J. Constr. Steel Res.*, **128**, 380-396. https://doi.org/10.1016/j.jcsr.2016.09.002.
Ishibuchi, H., Masuda, H., Tanigaki, Y. and Nojima, Y. (2015), "Modified distance calculation in generational distance and inverted generational distance", *Proceedings of the Evolutionary Multi-Criterion Optimization: 8th International Conference*, Guimarães, Portugal, March.
Kaveh, A. and Bakhshpoori, T. (2016), "An efficient multi-objective cuckoo search algorithm for design optimization", *Adv. Comput. Des.*, **1**(1), 87-103. http://doi.org/10.12989/acd.2016.1.1.087.
Kaveh, A. and Farhoudi, N. (2015), "Layout optimization of braced frames using differential evolution algorithm and dolphin echolocation optimization", *Periodica Polytechnica Civil Eng.*, **59**(3), 441-449. https://doi.org/10.3311/PPci.8155.
Kaveh, A. and Ilchi Ghazaan, M. (2016), "Truss optimization with dynamic constraints using UECBO", *Adv. Comput. Des.*, **1**(2), 119-138. http://doi.org/10.12989/acd.2016.1.2.119.
Kaveh, A. and Rezaei, M. (2016), "Topology and geometry optimization of different types of domes using ecbo", *Adv. Comput. Des.*, **1**(1), 1-25. http://doi.org/10.12989/acd.2016.1.1.001.
Kaveh, A., Vaez, S.R.H., Hosseini, P. and Ezzati, E. (2018), "Layout optimization of planar braced frames using modified dolphin monitoring operator", *Periodica Polytechnica Civil Eng.*, **62**(3), 717-731. ttps://doi.org/10.3311/PPci.11654.

Khaledy, N., Habibi, A. and Memarzadeh, P. (2019), "Multi-objective optimisation of steel moment frames subjected to blast", *Int. J. Struct.l Eng.*, **10**(1), 77-94. https://doi.org/10.1504/IJSTRUCTE.2019.101436.

Kicinger, R. and Arciszewski, T. (2004), "Multiobjective evolutionary design of steel structures in tall buildings", *Proceedings of the AIAA 1st Intelligent Systems Technical Conference*, Chicago, U.S.A., September.

Kicinger, R., Obayashi, S. and Arciszewski, T. (2007), "Evolutionary multiobjective optimization of steel structural systems in tall buildings", *Proceedings of the Evolutionary Multi-Criterion Optimization 4th International Conference*, Matsushima, Japan, March.

Kızılkan, M. (2010), "Investigating the effect of column orientations on minimum weight design of steel frames", Master's thesis, Middle East Technical University, Ancara, Turkey.

Kukkonen, S. and Lampinen, J. (2005), "GDE3: The third evolution step of generalized differential evolution", *Proceedings of the 2005 IEEE Congress on Evolutionary Computation*, Edinburgh, U.K., September.

Lemonge, A.C. and Barbosa, H.J. (2012), "Design optimization of space framed structures using multiple cardinality constraint", *Proceedings of the 3rd International Conference on Engineering Optimization*, Rio de Janeiro, Brazil, July.

Li, M., Zhen, L. and Yao, X. (2017), "How to read many-objective solution sets in parallel coordinates [educational forum]", *IEEE Comput. Intell. Magazine*, **12**(4), 88-100. https://doi.org/10.1109/MCI.2017.2742869.

Li, M., Burns, S.A. and Wen, Y.K. (2005), "Multiobjective optimization for performance-based seismic design of steel moment frame structures", *Earthq. Eng. Struct. Dyn.*, **34**(3), 289-306. https://doi.org/10.1061/40700(2004)148.

Mirjalili, S. and Lewis, A. (2016), "The whale optimization algorithm", *Adv. Eng. Softw.*, **95**, 51-67. https://doi.org/10.1016/j.advengsoft.2016.01.008.

Motta, J., Resende, C., Lemonge, A., Hallak, P. and Carvalho, J. (2021), "Optimal orientation of cross-sections of columns of 3D steel frames in a single and multi-objective optimization", *Proceedings of the XLII Ibero-Latin-American Congress on Computational Methods in Engineering*, Rio de Janeiro, Brazil, November.

Panagant, N., Bureerat, S. and Tai, K. (2019), "A novel self-adaptive hybrid multi-objective meta-heuristic for reliability design of trusses with simultaneous topology, shape and sizing optimisation design variables", *Struct. Multidiscipl. Opt.*, **60**(5), 1937-1955. https://10.1007/s00158-019-02302-x.

Papadrakakis, M., Lagaros, N. and Plevris, V. (2002), "Multi-objective optimization of skeletal structures under static and seismic loading conditions'", *Eng. Opt.*, **34**(6), 645-669. https://doi.org/10.1080/03052150215716.

Parreiras, R. and Vasconcelos, J. (2005), "Decision making in multiobjective optimization problems'", *ISE Book Series on Real Word Multi-Objective System Engineering*, Nova Science, New York, U.S.A., 1-20.

Parreiras, R. and Vasconcelos, J. (2009), "Decision making in multiobjective optimization aided by the multicriteria tournament decision method", *Nonlinear Anal. Theor.*, **71**(12), 191-198. https://doi.org/10.1016/j.na.2008.10.060.

Resende, C., Lemonge, A., Hallack, P., Carvalho, J. P. and Motta, J. (2020), "Global stability and natural frequencies of vibration in multi-objective op-timization of 3D steel frames", *Proceedings of the XLI Ibero-Latin-American Congress on Computational Methods in Engineering*, Foz do Iguaçu, Brazil, November.

Richardson, J.N., Nordenson, G., Laberenne, R., Coelho, R.F. and Adriaenssens, S. (2013), "Flexible optimum design of a bracing system for façade design using multiobjective genetic algorithms", *Auto. Constr.*, **32**, 80-87. https://doi.org/10.1016/j.autcon.2012.12.018.

Shen, W., Ohsaki, M. and Yamakawa, M. (2021), "Robust geometry and topology optimization of plane frames using order statistics and force density method with global stability constraint", *Int. J. Numer. Methods Eng.*, **122**(14), 3653-3677. https://doi.org/10.1002/nme.6676.

Storn, R. and Price, K. (1995), "Differential evolution-a simple and efficient adaptive scheme for global optimization over continuous spaces", tr-95-012, University of California, Berkeley, CA, U.S.A.

Tejani, G.G., Savsani, V.J., Patel, V.K. and Bureerat, S. (2017), “Topology, shape, and size optimization of truss structures using modified teaching-learning based optimization”, *Adv. Comput. Des.*, **2**(4), 313-331. https://doi.org/10.12989/acd.2017.2.4.313.

Tomei, V., Grande, E. and Imbimbo, M. (2022), “Design optimization of gridshells equipped with pre-tensioned rods”, *J. Build. Eng.*, **52**, 104407. https://doi.org/10.1016/j.jobe.2022.104407.

Tu, X., He, Z. and Huang, G. (2020), “Performance-based multi-objective collaborative optimization of steel frames with fuse-oriented buckling-restrained braces”, *Struct. Multidiscipl. Opt.*, **61**(1), 365-379. https://doi.org/10.1007/s00158-019-02366-9.

Wansasueb, K., Pholdee, N., Panagant, N. and Bureerat, S. (2022), “Multiobjective meta-heuristic with iterative parameter distribution estimation for aeroelastic design of an aircraft wing”, *Eng. Comput.*, **38**, 695-713. https://doi.org/10.1007/s00366-020-01077-w.

Yazdi H.M., Sulong, N. and Mosalman, F. (2010), “Fuzzy multi-objective genetic algorithm in determination of optimum mid connection location of off-centre bracing system”, *Proceedings of the 2010 3rd International Conference on Advanced Computer Theory and Engineering*, Chengdu, China, August.

Zitzler, E. and Thiele, L. (1999), “Multiobjective evolutionary algorithms: a comparative case study and the strengthpareto approach”, *IEEE T Evolution. Comput.*, **3**(4), 257-271. https://doi.org/10.1007/BFb0056872.

WT